VOL. 4, NO. 7, SEPTEMBER 2009 ISSN 1819-6608
ARPN Journal of Engineering and Applied Sciences


www.arpnjournals.com

FINITE ELEMENT SIMULATION OF IMPACTED FIBROUS COMPOSITE PANELS AND EFFICIENT PREDICTION OF TRANSVERSE SHEAR STRESSES

Umar Farooq and Karl Gregory
Built Environment and Engineering Department, University of Bolton, United Kingdom
E-Mail: uf1res@bolton.ac.uk, k.r.gregory@bolton.ac.uk

ABSTRACT

In this paper mathematical formulations and simulations were carried out for the prediction of through-thickness stress distributions of fibrous composite panels under variable shape impactors. Considerations were given to selective specimens from aerospace industrial environment to obtain the degree of uniformity of stress distributions throughout the out-of-plane geometry. The interlaminar stresses and strains induced in 'thin' laminates through application of membrane loads (i.e., in-plane loads) were also considered. Formulation was also developed for Poisson's ratios. Finite Element Method (FEM) has received a tremendous attention in engineering and industry because of its diversity and flexibility as an analysis tool. The solutions to physical problems can be obtained very effectively and to a high degree of accuracy using FEM software packages. Therefore, the FEM was chosen to perform simulation in commercially available software ABAQUS. In-plane stresses were computed from the model and Trapezium rule was applied to calculate out-of-plane transverse shear stresses. The procedure is simple and efficient to predict 3-D transverse shear stresses from 2-D model. Results were compared with the results from the available literature and found to be in good agreement. Some of the results are shown herein in the form of tables and graphs.

Keywords: model, fibrous composite panels, finite element analysis, through-thickness, transverse shear Stresses, velocity impact.

1. INTRODUCTION

The use of composites in light-weight advanced structures requires assessment of their damage tolerance. Efficient analytical tools, accurately predicting the behaviour of damage structures, are needed at the preliminary design stage in order to ensure their cost-effective performance.

All layer-wise models with the first order shear deformation theory depending on the number of layers are too expensive for practical applications and need continuous shape functions, a mixed/hybrid approach, or lead to non-conforming approximations.

Plate deformation theories can be divided in to two groups: stress based and displacement based theories. A brief review of displacement based theories is given below:

The first shear deformation theory was uniform proposed in [3-4]. According to the theory, transverse lines before deformation would be line after deformation but they were not normal to the mid-plane. The theory assumed constant transverse shear stress and it needed a shear correction factor in order to satisfy the plate boundary conditions on the lower and upper surface.

Different higher order theories were proposed in order to satisfy the plate boundary conditions. In [6-7] a transverse shear stress function in order to explain plate deformation was proposed. Later some new functions were proposed in [1, 2, 3 and 8]. Different shear deformation theories were compared for dynamic and static analysis of laminated composites in [9]. A higher order computational model for the free vibration analysis of anti-symmetric angle-ply plates in [10]. Studied static and free vibration and buckling of shear deformable composite laminates using mesh-free radial basis function method [11].

In recent years, the layer-wise theories and individual layer theories have been presented to obtain more accurate information on the ply level in [12-15]. However, these theories require numerous unknowns for multilayered plates and were often computationally expensive to obtain accurate results.

The displacement based plate finite element procedures are not capable of calculating accurate interfacial stresses. Three dimensional solid finite procedures are capable of calculating a detailed stress field when a sufficient number of elements are used. However, a three dimensional analysis poses practical problems in terms of computer memory usage and computation time requirements. The alternative approach, based on a hybrid finite element with independent displacement and stress approximations, leads to a higher order system of equations and results in practical problems in numerical implementation.

The need for through-thickness data poses a major problem; with the exception of shear, there are no recognized standards available for generating reliable design data. As a consequence, designers and engineers rely on in-plane data or ad hoc tests to determine structural performance. This approach is clearly unsatisfactory, as the use of the data will result in either under-designed or over-designed structures.

Therefore, there is a need for an efficient numerical analysis to calculate dynamic stress field in through-thickness in laminated composite structures. In-plane stresses from two-dimensional (2-D) plane analysis were used to predict transverse shear stresses and to

evaluate response to three-dimensional (3-D) loading configurations required for difficult but real aspects of design where the composites have to perform its function shaped (e.g. flanged) and connected (e.g. bonded) to the remainder of the system.

2. MATHEMATICAL FORMULATION STRATEGY

2.1. Displacement based equations

Displacement based shear deformation theory in [7] for N-plies:

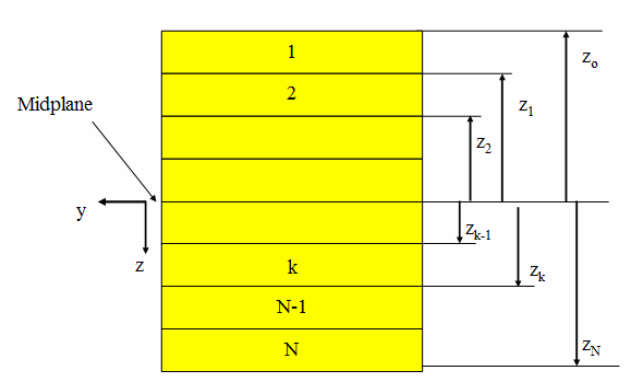

Figure-1. Configuration of N-ply lay-up.

The translational displacement of the mid-plane could be seen from the Figure-2 below while Figure-3 shows how in-plane u_o and v_o displacements are augmented by out-of-plane (Z-direction) displacements and rotations.

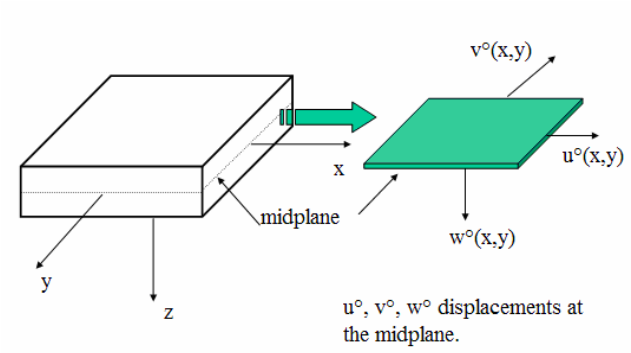

Figure-2. Translational displacement of the mid-plane.

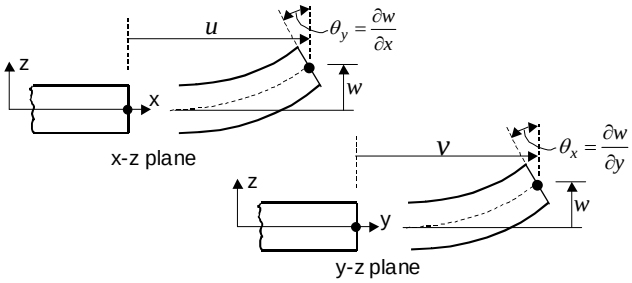

Figure-3. Bending displacement of the mid-plane.

The relations of displacements are given as,

$$u = u_o - z\frac{\partial w}{\partial x}, \; v = v_o - z\frac{\partial w}{\partial y},$$
$$\varepsilon_x = \frac{\partial u}{\partial x}, \; \varepsilon_y = \frac{\partial v}{\partial y}, \; \gamma_{xy} = \frac{\partial u}{\partial y} + \frac{\partial v}{\partial x} \quad (1)$$

From Eq. (2) the strain-displacement relationship are rewritten here for components of displacement, u and v, confined to the x-y plane ("in-plane"). A similar expression for twist, k_{xy}, can be derived for twist is defined as an "angular change" per "unit length".

$$k_{xy} = -2\frac{\partial^2 w}{\partial x \partial y}, \quad \begin{Bmatrix} \varepsilon_x \\ \varepsilon_y \\ \gamma_{xy} \end{Bmatrix} = \begin{Bmatrix} \varepsilon_x^o \\ \varepsilon_y^o \\ \gamma_{xy}^o \end{Bmatrix} + \begin{Bmatrix} k_x \\ k_y \\ k_{xy} \end{Bmatrix} \quad (2)$$

Where u, v, w_1 are the unknown displacement functions of middle surface of the plate while shape functions determining the distribution of the transverse shear strains and stresses along the thickness.

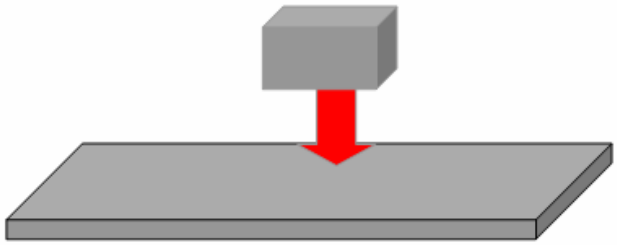

Figure-4. Schematic of a laminated plate under out-of-plane blunt nose impactor.

The classical plate equations arise from a combination of four distinct subsets of plate theory: the kinematics, constitutive, force resultant, and equilibrium equations. The same analogy applies in modeling fibrous composite panels. To relate the plate's out-of-plane displacement w0 to its pressure loading pz, it combines the results of the four plate subcategories in this order:

Kinematics -> Constitutive -> Resultants -> Equilibrium = Plate Equation

Traditionally, volume force is denoted by p and line force by q. If forces are acting on a domain from an external source these are called external forces. The general stress components acting on an infinitesimal element are shown in Figure-3.

$$\frac{\partial \sigma_x}{\partial x}+\frac{\partial \sigma_{xy}}{\partial y}+\frac{\partial \sigma_{xz}}{\partial z}+p_x=\rho\frac{\partial^2 u}{\partial t^2}$$
$$\frac{\partial \sigma_{yx}}{\partial x}+\frac{\partial \sigma_y}{\partial y}+\frac{\partial \sigma_{yz}}{\partial z}+p_y=\rho\frac{\partial^2 v}{\partial t^2}$$
$$\frac{\partial \sigma_{zx}}{\partial x}+\frac{\partial \sigma_{zy}}{\partial y}+\frac{\partial \sigma_z}{\partial z}+p_z=\rho\frac{\partial^2 w}{\partial t^2} \quad (3)$$

2.2. Through-thickness properties: Poisson's ratios

We begin with the definition of this through-thickness Poisson's ratio υ_{xz} and υ_{yz} in terms of the through-thickness strain ε_z and the in-plane strain ε_x in the direction of the applied load, i.e.,

$$\nu_{xz}=-\frac{\varepsilon_z}{\varepsilon_x} \quad (4)$$

For the loading Nx ≠ 0 which with all other applied forces and moments being zero. The average (or overall) through-thickness strain ε_z can be written in terms of the total change in thickness, Δw, divided by the laminate thickness 2H

$$\varepsilon_z=\frac{\Delta w}{2H} \quad (5)$$

The total thickness change can be written as the integral of the displacement $\varepsilon_z dz$ over the thickness of the laminate:

$$\Delta w=\int_{-H}^{H}\varepsilon_z dz \quad (6)$$

For uniform plane stress in each layer of the laminate, the through-thickness strain ε_z^k constant in any kth layer can be determine from the 3-D Hooke's law:

$$\varepsilon_x=\bar{S}_{11}\sigma_x+\bar{S}_{12}\sigma_y+\bar{S}_{13}\sigma_z+\bar{S}_{16}\tau_{xy}$$
$$\varepsilon_y=\bar{S}_{12}\sigma_x+\bar{S}_{22}\sigma_y+\bar{S}_{23}\sigma_z+\bar{S}_{26}\tau_{xy}$$
$$\varepsilon_z=\bar{S}_{13}\sigma_x+\bar{S}_{23}\sigma_y+\bar{S}_{33}\sigma_z+\bar{S}_{36}\tau_{xy}$$
$$\gamma_{yz}=\bar{S}_{44}\tau_{yz}+\bar{S}_{45}\tau_{zx}$$
$$\gamma_{zx}=\bar{S}_{45}\tau_{yz}+\bar{S}_{55}\tau_{zx}$$
$$\gamma_{xy}=\bar{S}_{16}\sigma_x+\bar{S}_{26}\sigma_y+\bar{S}_{36}\sigma_z+\bar{S}_{66}\tau_{xy}$$
$$\varepsilon_z^k=\bar{S}_{13}^k\sigma_x^k+\bar{S}_{23}^k\sigma_y^k+\bar{S}_{36}^k\tau_{xy}^k \quad (7)$$

The stresses in from the plane stress constitutive are:

$$\begin{Bmatrix}\sigma_x\\ \sigma_y\\ \tau_{xy}\end{Bmatrix}=\begin{bmatrix}\bar{Q}_{11} & \bar{Q}_{12} & \bar{Q}_{16}\\ \bar{Q}_{12} & \bar{Q}_{22} & \bar{Q}_{26}\\ \bar{Q}_{16} & \bar{Q}_{26} & \bar{Q}_{66}\end{bmatrix}\begin{Bmatrix}\varepsilon_x\\ \varepsilon_y\\ \gamma_{xy}\end{Bmatrix} \quad (8)$$

For the k[th] layer

$$\begin{Bmatrix}\sigma_x\\ \sigma_y\\ \tau_{xy}\end{Bmatrix}_k=\begin{bmatrix}\bar{Q}_{11} & \bar{Q}_{12} & \bar{Q}_{16}\\ \bar{Q}_{12} & \bar{Q}_{22} & \bar{Q}_{26}\\ \bar{Q}_{16} & \bar{Q}_{26} & \bar{Q}_{66}\end{bmatrix}_k\begin{Bmatrix}\varepsilon_x\\ \varepsilon_y\\ \gamma_{xy}\end{Bmatrix}_k \quad (9)$$

Now, for a symmetric laminate subjected to the in-plane loading Nx, NY = Nxy = 0, and {M} = 0, the strains in the kth layer are

$$\begin{Bmatrix}\varepsilon_x\\ \varepsilon_y\\ \gamma_{xy}\end{Bmatrix}^k=\begin{Bmatrix}\varepsilon_x^0\\ \varepsilon_y^0\\ \gamma_{xy}^0\end{Bmatrix}=A^{-1}\begin{Bmatrix}N_x\\ 0\\ 0\end{Bmatrix} \quad (10)$$

Combining the through-thickness strains in the kth layer:

$$\begin{Bmatrix}\sigma_x\\ \sigma_y\\ \tau_{xy}\end{Bmatrix}_k=\begin{bmatrix}\bar{Q}_{11} & \bar{Q}_{12} & \bar{Q}_{16}\\ \bar{Q}_{12} & \bar{Q}_{22} & \bar{Q}_{26}\\ \bar{Q}_{16} & \bar{Q}_{26} & \bar{Q}_{66}\end{bmatrix}_k\begin{Bmatrix}A_{11}^{-1}\\ A_{12}^{-1}\\ A_{16}^{-1}\end{Bmatrix}_k N_x \quad (11)$$

Gives:

$$\varepsilon_z^k=N_x\begin{bmatrix}A_{11}^{-1}\left(\bar{S}_{13}^k\bar{Q}_{11}^k+\bar{S}_{23}^k\bar{Q}_{12}^k+\bar{S}_{36}^k\right)+\\ A_{12}^{-1}\left(\bar{S}_{13}^k\bar{Q}_{12}^k+\bar{S}_{23}^k\bar{Q}_{22}^k+\bar{S}_{36}^k\bar{Q}_{26}^k\right)+\\ A_{16}^{-1}\left(\bar{S}_{13}^k\bar{Q}_{16}^k+\bar{S}_{23}^k\bar{Q}_{26}^k+\bar{S}_{36}^k\bar{Q}_{66}^k\right)\end{bmatrix} \quad (12)$$

Prescribed loading thus to give the total change in laminate thickness:

$$\Delta w=N_x\left(A_{11}^{-1}F_1+A_{12}^{-1}F_2+A_{16}^{-1}F_6\right) \quad (13)$$

Where the Fi are defined as

$$F_i=\sum_{k=1}^{N}\left[\left(\bar{S}_{13}^k\bar{Q}_{1i}^k+\bar{S}_{23}^k\bar{Q}_{2i}^k+\bar{S}_{36}^k\bar{Q}_{6i}^k\right)t_k\right] \qquad (i=1,2,6) \quad (14)$$

Finally, becomes

$$\nu_{xz}=-\frac{\left(A_{11}^{-1}F_1+A_{12}^{-1}F_2+A_{16}^{-1}F_6\right)}{2HA_{11}^{-1}} \quad (15)$$

Or more simply

$$\nu_{xz}=-\frac{A_{1i}^{-1}F_i}{2HA_{11}^{-1}} \qquad (i=1,2,6) \quad (16)$$

In a similar fashion, it can be shown that the through-thickness Poisson's ratios υ_{yz} for loading in the y-direction is

$$\nu_{yz} = \frac{A_2^1 F_i}{2HA_{22}^1} \qquad (i = 1,2,6) \tag{17}$$

2.3. Formulation of transverse shear effects

The basic approaches as summarized by a symmetric laminates with orthotropic laminate having principal material directions aligned with the plate axes are treated. The transverse normal strain can be found from the orthotropic stress-strain relations as

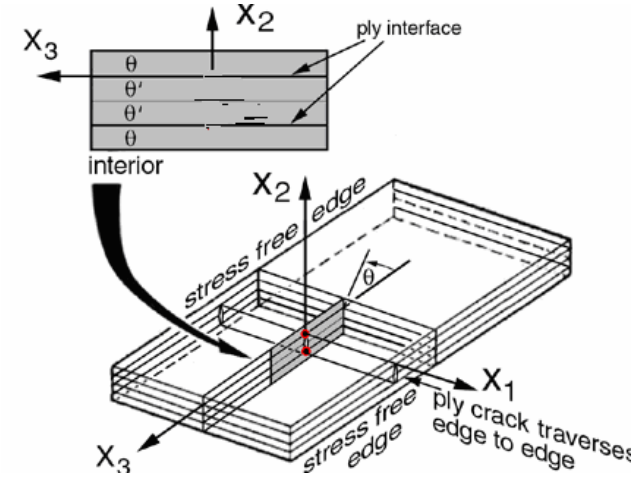

Figure-5. Transverse shear stresses at edges.

$$\varepsilon_z = \frac{1}{C_{33}}\left(\sigma_z - C_{13}\,\varepsilon_x - C_{23}\,\varepsilon_y\right) \tag{18}$$

Which can be used to eliminate ez from the stress-strain relations for the kth layer, leaving

$$\begin{bmatrix}\sigma_x\\ \sigma_y\\ \tau_{yz}\\ \tau_{xz}\\ \tau_{xy}\end{bmatrix}_k = \begin{bmatrix}Q_{11} & Q_{12} & 0 & 0 & 0\\ Q_{12} & Q_{22} & 0 & 0 & 0\\ 0 & 0 & Q_{44} & 0 & 0\\ 0 & 0 & 0 & Q_{55} & 0\\ 0 & 0 & 0 & 0 & Q_{66}\end{bmatrix}_k \begin{bmatrix}\varepsilon_x\\ \varepsilon_y\\ \gamma_{yz}\\ \gamma_{xz}\\ \gamma_{xy}\end{bmatrix}_k \tag{19}$$

Where, if σ_z is neglected as in classical lamination theory,

$$Q_{ij} = \begin{cases} C_{ij} - \dfrac{C_{i3}C_{j3}}{C_{33}}, \text{ if i, j} = 1,2 \\ C_{ij}, \text{ if i, j} = 4,5,6 \end{cases} \tag{20}$$

The transverse shear stress distribution is then approximated by

$$\tau_{xz}^k = \left[Q_{55}^k\, f(z) + a_{55}^k\right]\phi_x(x,y)$$
$$\tau_{yz}^k = \left[Q_{44}^k\, f(z) + a_{44}^k\right]\phi_y(x,y) \tag{21}$$

Where f (z) = f (-z) because of laminate symmetry. Also, and are determined from the equilibrium conditions that the shearing stresses vanish at the top and bottom surfaces of the plate [f (t/2) = f (-t/2) = 0] and are continuous as layer interface. The shearing strains are obtained from the stress-strain relations as

$$\gamma_{xz}^k = \left[f(z) + \frac{a_{55}^k}{Q_{55}^k}\right]\phi_x \tag{22}$$

$$\gamma_{yz}^k = \left[f(z) + \frac{a_{44}^k}{Q_{44}^k}\right]\phi_y \tag{23}$$

Then, integration of the strain-displacement relation, Eq. (23), with respect to z (with w assumed to be independent of z) yields

$$u^k = -zw_{,x} + \left[J(z) + g_1^k(z)\right]\phi_x$$
$$v^k = -zw_{,y} + \left[J(z) + g_2^k(z)\right]\phi_y \tag{24}$$

Where

$$J(z) = \int f(z)\,dz \qquad g_1^k(z) = \frac{a_{55}^k}{Q_{55}^k}z + b_1^k$$

$$g_2^k(z) = \frac{a_{44}^k}{Q_{44}^k}z + b_2^k \tag{25}$$

The constants b_1^k and b_2^k are found to from continuity conditions for u and v at the layer interfaces and the symmetry condition that u and v vanish at the laminate middle surface. Obviously, because of the presence of Φ_x and Φ_y, u and v are not linear functions of z as in classical lamination theory.

The moment relations are obtained from integration of the strain relations, Eq. (20) after the strain-displacement relations, Equation and the displacement relations, equation-are the displacement relations, Equation are substituted:

$$M_x = -D_{11}w_{,xx} - D_{12}w_{,yy} + \left(F_{11} + H_{11}\right)\phi_{x,x} + \left(F_{12} + H_{122}\right)\phi_{y,y}$$
$$M_y = -D_{12}w_{,xx} - D_{22}w_{,yy} + \left(F_{12} + H_{121}\right)\phi_{x,x} + \left(F_{22} + H_{222}\right)\phi_{y,y}$$
$$M_{xy} = -2D_{66}w_{,xy} + \left(F_{66} + H_{661}\right)\phi_{x,y} + \left(F_{66} + H_{662}\right)\phi_{y,x} \tag{26}$$

Where the D_{ij} are the usual bending stiffness and

$$F_{ij} = \int_{-\frac{t}{2}}^{\frac{t}{2}} Q_{ij}^k\, zJ(z)\,dz \qquad \text{i,j} = 1, 2, 6 \tag{27}$$

$$H_{ijl} = \int_{-\frac{t}{2}}^{\frac{t}{2}} Q_{ij}^k\, zg_l^k(z)\,dz \qquad 1 = 1, 2 \tag{28}$$

The shear resultants are

$$Q_x = \int_{-\frac{t}{2}}^{\frac{t}{2}} \tau_{xz}^k \, dz = K_{55} \, \phi_x$$

$$Q_y = \int_{-\frac{t}{2}}^{\frac{t}{2}} \tau_{yz}^k \, dz = K_{44} \, \phi_y \quad (29)$$

Where

$$K_{ii} = \int_{-\frac{t}{2}}^{\frac{t}{2}} \left[Q_{ii}^k \; f(z) + a_{ii}^k \right] dz \quad \text{i} = 4, 5 \quad (30)$$

The large-deflection equilibrium equations are

$$M_{x,x} + M_{xy,y} - Q_x = 0$$
$$M_{xy,x} + M_{y,y} - Q_y = 0$$

$$Q_{x,x} + Q_{y,y} + p + N_x w_{,xx} + 2N_{xy} w_{,xy} + N_y w_{,yy} = 0 \quad (31)$$

Or, in terms of the present variables,

$$\begin{aligned}
&D_{11} w_{,xxx} + (D_{12} + 2D_{66}) w_{,xyy} - (F_{11} + H_{111}) \phi_{x,xx} \\
&- (F_{66} + H_{661}) \Phi_{x,yy} \\
&- (F_{12} + F_{66} + H_{122} + H_{662}) \phi_{y,xy} + K_{55} \phi_x = 0 \\
&(D_{12} + 2D_{66}) w_{,xxy} + D_{22} w_{,yyy} \\
&+ (F_{12} + F_{66} + H_{121} + H_{661}) \phi_{x,xy} \\
&+ (F_{66} + H_{662}) \Phi_{y,xx} + (F_{22} + H_{222}) \phi_{y,yy} + K_{44} \phi_y = 0 \\
&K_{55} \phi_{x,x} + K_{44} \phi_{y,y} + p + N_x w_{,xx} \\
&+ 2N_{xy} w_{,xy} + N_y w_{,yy} = 0
\end{aligned} \quad (32)$$

Then, the overall problem is determined and reduces to the solution of the following set of simultaneous algebraic equations for A, B, and C from Eq. (6) becomes:

$$\begin{aligned}
&\left[D_{11} m^2 + (D_{12} + 2D_{66}) n^2 R^2 \right] \left[\frac{m\pi}{a} \right] A - \left[(F_{11} + H_{111}) m^2 + (F_{66} + H_{661}) n^2 R^2 + \frac{K_{55} R^2 S^2}{\pi^2} \right] B - (F_{12} + F_{66} + H_{122} + H_{662}) mnRC = 0 \\
&\left[(D_{12} + 2D_{66}) m^2 + D_{22} n^2 R^2 \right] \left[\frac{n\pi R}{a} \right] A - (F_{121} + F_{66} + H_{121} + H_{661}) \, mn \, RB - \left[(F_{66} + H_{662}) m^2 + (F_{22} + H_{222}) n^2 R^2 + \frac{K_{44} R^2 S^2}{\pi^2} \right] C = 0
\end{aligned} \quad (33)$$

2.4. Load stress relationships

Normal, tangential, and axial forces may act on the surface, and the body forces may act parallel and normal to the longitudinal axis. In addition, an axial force, moment, and torque may be applied at the ends. The forces acting perpendicular and parallel to the longitudinal axis are referred to as in-plane and out-of-plane. When two or more types of loads are applied, the stresses and strains can independently be calculated for each type of load. The stresses and strains thus obtained are then superimposed to obtain the final results. Plane-strain condition requires that the strains do not vary along the longitudinal axis, thus, in the x, y, z coordinate system we have

$$\frac{\partial \varepsilon_x}{\partial z} = 0 \; \frac{\partial \varepsilon_y}{\partial z} = 0 \; \frac{\partial \varepsilon_z}{\partial z} = 0; \; \frac{\partial \gamma_{yz}}{\partial z} = 0 \; \frac{\partial \gamma_{xz}}{\partial z} = 0 \; \frac{\partial \gamma_{xy}}{\partial z} = 0 \quad (33)$$

The following displacements satisfy these conditions

$$\begin{aligned}
u &= U(x, y) - C_1 yz - \frac{1}{2} C_2 z^2 \\
v &= V(x, y) + C_1 xz - \frac{1}{2} C_3 z^2 \\
w &= W(x, y) + (C_2 x + C_3 y + C_4) z
\end{aligned} \quad (34)$$

Where U, V, and W are functions that depend on x and y, and C_1, C_2, C_3, and C_4 are constants. For small displacements we have the following relationships:

$$\varepsilon_z^0 = \frac{\partial w}{\partial z} \quad \frac{1}{\rho_y} = -\frac{\partial^2 u}{\partial z^2} \quad \frac{1}{\rho_x} = -\frac{\partial^2 v}{\partial z^2} \quad (35)$$

Where ε_z^0 is the strain along the longitudinal axis?

$\frac{1}{\rho_y}$, $\frac{1}{\rho_x}$ Are the curvatures of the longitudinal axis in the x-z and y-z planes, respectively? By virtue of $\frac{\partial \gamma_{xy}}{\partial z} = 0$, it gives $\frac{\partial^2 u}{\partial y \, \partial z} + \frac{\partial^2 v}{\partial x \, \partial z} = 0$ and $\vartheta \equiv \frac{\partial}{\partial z}\left(\frac{\partial v}{\partial x}\right) = -\frac{\partial}{\partial z}\left(\frac{\partial u}{\partial y}\right)$ could be defined.

The ϑ represent the rate of twist of the cross-section.

The constants are determined from

$\vartheta \equiv \frac{\partial}{\partial z}\left(\frac{\partial v}{\partial x}\right) = -\frac{\partial}{\partial z}\left(\frac{\partial u}{\partial y}\right) = C_1$ the strain equations can be written as

$$\varepsilon_z^0 = \frac{\partial w}{\partial z} = C_4; \frac{1}{\rho_y} = -\frac{\partial^2 u}{\partial z^2} = C_2; \frac{1}{\rho_x} = -\frac{\partial^2 v}{\partial z^2} = C_3 \quad (36)$$

And displacements can be written as

$$u = U(x,y) - \vartheta yz - \frac{1}{2}\frac{1}{\rho_y}z^2$$
$$v = V(x,y) + \vartheta xz - \frac{1}{2}\frac{1}{\rho_x}z^2 \quad (37)$$
$$w = W(x,y) + (\frac{1}{\rho_y}x + \frac{1}{\rho_x}y + \varepsilon_z^0)z$$

Deformations and displacements under plane-strain condition. In the x_1, x_2, x_3 coordinate system u, v, w are replaced by u_1, u_2, u_3; U, V, W by U_1, U_2, U_3; and by ρ_x, ρ_y by ρ_1, ρ_2. The u, v, w components of the displacements corresponding to the each of the deformations. Again use the x, y, z coordinate system for generally anisotropic materials. For monoclinic, orthotropic, transversally isotropic, and isotropic materials we use the x_1, x_2, x_3 coordinate system, with x_3 being along the longitudinal axis of the body. In the x_1, x_2, x_3 coordinate system the displacements are

$$u_1 = U_1(x_1,x_2) - \vartheta x_2 x_3 - \frac{1}{2}\frac{1}{\rho_2}x_3^2$$
$$u_2 = U_2(x_1,x_2) + \vartheta x_1 x_3 - \frac{1}{2}\frac{1}{\rho_1}x_3^2 \quad (38)$$
$$u_3 = U_3(x_1,x_2) + (\frac{1}{\rho_2}x_1 + \frac{1}{\rho_1}x_2 + \varepsilon_3^0)x_3$$

Where ε_z^0 is the strain along longitudinal axis: $\frac{1}{\rho_2}$, $\frac{1}{\rho_1}$ are the curvatures of this axis in the x_1-x_3 and x_2-x_3 planes, respectively; υ represents the rate of twist of the cross section. Shear stresses were calculated from Eqs (23) and (25).

3. FINITE ELEMENT MODEL SETTING UP

Composite laminates of diameter 23.94 mm, with stacking sequences $[45/0/-45/90]_S$ and $[45/0/-45/90]_{3S}$ the effect of impact duration, length and position on the impact loads were studied with 2.88 mm thickness of quasi-isotropic configuration under centrally located load at circle of 6.3 mm diameter was studied for various data input and stacking sequences and clamped boundary conditions.

The developed model to predict the composite structure behaviour and implemented into software ABAQUS™ are shown in Figure-7 below.

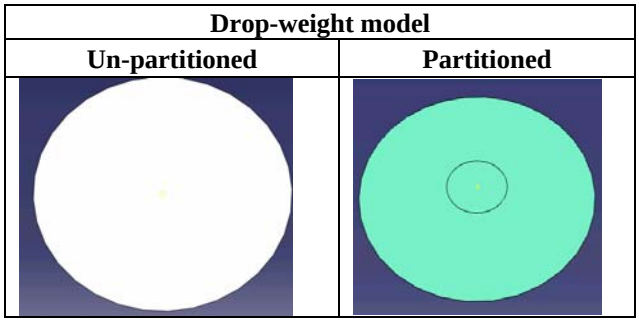

Figure-6. Models for simulation.

The properties of a unidirectional lamina of specimens with geometries and data are given in Table-1.

Table-1. Material and geometrical input data.

Material properties	Ultimate strengths	Stacking sequences
E_1 = 150 GPa, E_2 = E_3 = 15 GPa	$(\sigma_1^T)_{ult}$ = 1500 MPa	$[45/0/-45/90]_S$,
G_{12} = 5.7 GPa G_{13} = 5.7 Gpa G23 =7.26 GPa	$(\sigma_2^T)_{ult}$ = = 40 MPa	
Poisson's Ratios ν_{12} = 0.33 ν_{23} = 0.03 ν_{13} = 0.01	$(\sigma_2^C)_{ult}$ = 20 MPa	$[45/0/-45/90]3_S$
	$(\tau_{12})_{ult}$ = 53 MPa	

The computational model was developed for this analysis: a static analysis was performed to calibrate the finite element model. An arbitrary load of 16 kN was applied to the top surface and both axial and rotational restraints were applied to the edge boundaries as illustrated in the Figure-7. The material properties were assigned to the impactor and the specimen, the local element orientation was defined in terms of the global *X, Y* and *Z* axes. Each layer of elements through the thickness was treated as a single ply although they actually as previously mentioned accounted for three plies. Simulation for overall laminate stiffness of each ply in the model rotated to align the major ply mechanical properties with the principal fibre directions in the code.

The composite lay-up and impactor were assembled in the assembly module. In the Step module Explicit Dynamic was chosen for this analysis and impact duration was set to 1.1 μs.

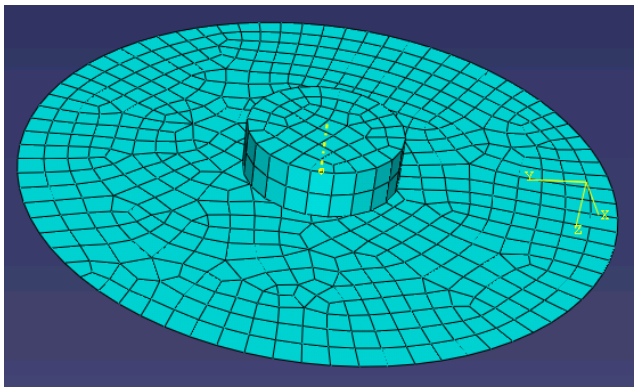

Figure 7: Meshed model using finite elements: (a) Shell element S4 and (b) Solid element C3D8 for impactor.

4. NUMERICAL RESULTS AND DISCUSSIONS

A computational model was developed in the commercially available software ABAQUS. In-plane stresses were predicted by the model and recorded for post-processing calculations of transverse shear stresses. Three configurations of 24, 15, and 8 plies were tested and their results were compared. Results from the model consisting of 24 plies were selected to include herein. Transverse stresses from mathematical formulations were calculated for three points 10, 92, and 118 were selected for each and every ply of the model to record the results and shown in Table-3 and 4 above. In-plane stresses were used along with the Trapezoidal rule to calculate through the thickness stresses and were shown in table 5 above. Graphs of the transverse shear stresses were also drawn and shown for the same data. The tabular results and graphs shown above prove that the results obtained from the computations are real within the limits and reliable.

Computer generated results are presented in tabular, graphs and contour plots. These results provided information as a basis to build analysis for the composite panels subjected to impacts from various nose impactors. These results are for stacking sequences $[45/0/-45/90]_{S,}$ $[45/0/-45/90]_{2s}$ and $[45/0/-45/90]_{3S.}$ The effect of impactor's shape for impact duration, length and position on the impact velocities and loads were studied. Based on the illustration and prior experience, a shortened procedure was to select results for one set-up for discussion with sizing and ranking procedure is based on FPF.

Selected results for $[45/0/-45/90]_6$ lay-up run in the three models were considered and compared. Given the fixed ply thickness for the material results for acceleration, velocities, displacements, stresses and strains were shown in the Table-2. Shows time steps and duration for which amplitudes velocities or loads used to impact the models. Tables 3 to 6 show the predicted results for transverse stresses and their calculation from 2-D data.

Table-2. Time and 5 amplitudes of velocities and loads.

Time	**Amplitudes** (non-dimensional)				
	1	2	3	4	5
0	0.05	0.05	0.02	0.05	0.05
5.50E-05	0.08	0.05	0.02	0.1	0.1
0.00011	0.15	0.06	0.03	0.2	0.1
0.000165	0.3	0.1	0.04	0.3	0.1
0.00022	0.4	0.2	0.05	0.4	0.1
0.000275	0.5	0.3	0.1	0.5	0.2
0.00033	0.6	0.4	0.2	0.6	0.2
0.000385	0.7	0.5	0.3	0.7	0.2
0.00044	0.8	0.6	0.4	0.8	0.3
0.000495	0.9	0.8	0.5	0.9	0.8
0.00055	1	0.9	0.6	1	0.9
0.000605	0.9	1	0.7	0.9	1
0.00066	0.8	0.9	0.8	0.8	0.9
0.000715	0.6	0.8	0.9	0.7	0.8
0.00077	0.5	0.7	1	0.6	0.3
0.000825	0.4	0.6	0.9	0.5	0.3
0.00088	0.3	0.5	0.8	0.4	0.2
0.000935	0.3	0.4	0.7	0.4	0.2
0.00099	0.2	0.2	0.6	0.3	0.2
0.001045	0.2	0.3	0.5	0.3	0.2
0.0011	0.2	0.3	0.4	0.3	0.2

Table-3. Predicted stresses in x-x direction.

Ply No.	Z-Dist	Node 1	Node 2	Difference	Diff stresses	Z-Dir stresses	Trapz rule
	Mm	118	10				
1	0.12	2.57E+08	5.65E+08	3.08E+08	3.22E+11	6.63E+11	3.97E+07
2	0.24	2.57E+08	5.84E+08	3.26E+08	3.41E+11	4.22E+11	2.53E+07
3	0.36	3.69E+07	1.14E+08	7.77E+07	8.11E+10	1.43E+11	8.59E+06
4	0.48	3.65E+07	9.60E+07	5.95E+07	6.21E+10	3.84E+11	2.30E+07
5	0.6	2.57E+08	5.65E+08	3.08E+08	3.22E+11	6.63E+11	3.97E+07
6	0.72	2.57E+08	5.84E+08	3.26E+08	3.41E+11	4.22E+11	2.53E+07
7	0.84	3.69E+07	1.14E+08	7.77E+07	8.11E+10	1.43E+11	8.59E+06
8	0.96	3.65E+07	9.60E+07	5.95E+07	6.21E+10	3.84E+11	2.30E+07
9	1.08	2.57E+08	5.65E+08	3.08E+08	3.22E+11	6.63E+11	3.97E+07
10	1.20	2.57E+08	5.84E+08	3.26E+08	3.41E+11	4.22E+11	2.53E+07
11	1.32	3.69E+07	1.14E+08	7.77E+07	8.11E+10	1.43E+11	8.59E+06
12	1.44	3.65E+07	9.60E+07	5.95E+07	6.21E+10	1.24E+11	7.45E+06
13	1.56	3.65E+07	9.60E+07	5.95E+07	6.21E+10	-1.8E+10	-1.13E+06
14	1.68	-3.69E+07	-1.146E+08	-7.77E+07	-8.10E+10	-4.2E+11	-2.53E+07
15	1.80	-2.57E+08	-5.84E+08	-3.26E+08	-3.40E+11	-6.6E+11	-3.97E+07
16	1.92	-2.57E+08	-5.65E+08	-3.08E+08	-3.22E+11	-3.8E+11	-2.30E+07
17	2.04	-3.65E+07	-9.60E+07	-5.95E+07	-6.21E+10	-1.4E+11	-8.59E+06
16	2.16	-3.69E+07	-1.146E+08	-7.77E+07	-8.10E+10	-4.2E+11	-2.53E+07
19	2.28	-2.57E+08	-5.84E+08	-3.26E+08	-3.40E+11	-6.6E+11	-3.97E+07
20	2.40	-2.57E+08	-5.65E+08	-3.08E+08	-3.22E+11	-3.8E+11	-2.30E+07
21	2.52	-3.65E+07	-9.60E+07	-5.95E+07	-6.21E+10	-1.4E+11	-8.59E+06
22	2.64	-3.69E+07	-1.14E+08	-7.77E+07	-8.10E+10	-4.2E+11	-2.53E+07
23	2.76	-2.57E+08	-5.84E+08	-3.26E+08	-3.40E+11	-6.6E+11	-3.97E+07
24	2.88	-2.57E+08	-5.65E+08	-3.08E+08	-3.22E+11	-3.2E+11	-1.93E+07

Table-4. Predicted stresses in y-y direction.

Ply	Z-Dist	Node 1: 118	Node 2: 92	Difference	Diff stresses	Z-Dir stresses	Trapz rule
1	0.12	2.35E+07	2.92E+07	5.69E+06	6.97E+09	7.93E+09	4.76E+05
2	0.24	2.34E+07	2.42E+07	7.81E+05	9.57E+08	1.48E+09	8.88E+04
3	0.36	6.03E+07	6.08E+07	4.27E+05	5.23E+08	7.06E+09	4.23E+05
4	0.48	6.04E+07	6.57E+07	5.33E+06	6.53E+09	1.35E+10	8.11E+05
5	0.6	2.35E+07	2.92E+07	5.69E+06	6.97E+09	7.93E+09	4.76E+05
6	0.72	2.34E+07	2.42E+07	7.81E+05	9.57E+08	1.48E+09	8.88E+04
7	0.84	6.03E+07	6.08E+07	4.27E+05	5.23E+08	7.06E+09	4.23E+05
8	0.96	6.04E+07	6.57E+07	5.33E+06	6.53E+09	1.35E+10	8.11E+05
9	1.08	2.35E+07	2.92E+07	5.69E+06	6.97E+09	7.93E+09	4.76E+05
10	1.20	2.34E+07	2.42E+07	7.81E+05	9.57E+08	1.48E+09	8.88E+04
11	1.32	6.03E+07	6.08E+07	4.27E+05	5.23E+08	7.06E+09	4.23E+05
12	1.44	6.04E+07	6.57E+07	5.33E+06	6.53E+09	1.30E+10	7.84E+05
13	1.56	6.04E+07	6.57E+07	5.33E+06	6.53E+09	6.01E+09	3.60E+05
14	1.68	-6.03E+07	-6.08E+07	-4.27E+05	-5.23E+08	-1.4E+09	-8.88E+04
15	1.80	-2.340E+07	-2.42E+07	-7.81E+05	-9.56E+08	-7.9E+09	-4.76E+05
16	1.92	-2.35E+07	-2.92E+07	-5.69E+06	-6.97E+09	-1.3E+10	-8.10E+05
17	2.04	-6.04E+07	-6.57E+07	-5.33E+06	-6.53E+09	-7.0E+09	-4.23E+05
16	2.16	-6.03E+07	-6.08E+07	-4.27E+05	-5.23E+08	-1.4E+09	-8.88E+04
19	2.28	-2.34E+07	-2.42E+07	-7.81E+05	-9.56E+08	-7.9E+09	-4.76E+05
20	2.40	-2.35E+07	-2.92E+07	-5.69E+06	-6.97E+09	-1.3E+10	-8.10E+05
21	2.52	-6.04E+07	-6.57E+07	-5.33E+06	-6.53E+09	-7.0E+09	-4.23E+05
22	2.64	-6.03E+07	-6.08E+07	-4.27E+05	-5.23E+08	-1.4E+09	-8.88E+04
23	2.76	-2.34E+07	-2.42E+07	-7.81E+05	-9.56E+08	-7.9E+09	-4.76E+05
24	2.88	-2.35E+07	-2.92E+07	-5.69E+06	-6.97E+09	-6.9E+09	-4.18E+05

Table-5. Stresses calculated from Table-3 and Table-4.

Ply	Z-Dist	Node 1: 118	Node 2: 10	Difference	Diff stresses	Z-Dir stresses	Trapz rule
1	0.12	-2.04E+07	-4.51E+07	-2.47E+07	-2.58E+10	-3.5E+09	-2.10E+05
2	0.24	2.03E+07	4.17E+07	2.13E+07	2.22E+10	4.80E+10	2.88E+06
3	0.36	2.04E+07	4.51E+07	2.47E+07	2.58E+10	3.51E+09	2.10E+05
4	0.48	-2.03E+07	-4.17E+07	-2.13E+07	-2.22E+10	-4.8E+10	-2.88E+06
5	0.6	-2.04E+07	-4.51E+07	-2.47E+07	-2.58E+10	-3.5E+09	-2.10E+05
6	0.72	2.03E+07	4.17E+07	2.13E+07	2.22E+10	4.80E+10	2.88E+06
7	0.84	2.04E+07	4.51E+07	2.47E+07	2.58E+10	3.51E+09	2.10E+05
8	0.96	-2.03E+07	-4.17E+07	-2.13E+07	-2.22E+10	-4.8E+10	-2.88E+06
9	1.08	-2.04E+07	-4.51E+07	-2.47E+07	-2.58E+10	-3.5E+09	-2.10E+05
10	1.20	2.03E+07	4.17E+07	2.13E+07	2.22E+10	4.80E+10	2.88E+06
11	1.32	2.04E+07	4.51E+07	2.47E+07	2.58E+10	3.51E+09	2.10E+05
12	1.44	-2.03E+07	-4.17E+07	-2.13E+07	-2.22E+10	-4.4E+10	-2.67E+06
13	1.56	-2.03E+07	-4.17E+07	-2.13E+07	-2.22E+10	-4.8E+10	-2.88E+06
14	1.68	-2.04E+07	-4.51E+07	-2.47E+07	-2.58E+10	-4.8E+10	-2.88E+06
15	1.80	-2.03E+07	-4.17E+07	-2.13E+07	-2.22E+10	3.51E+09	2.10E+05
16	1.92	2.04E+07	4.51E+07	2.47E+07	2.58E+10	4.80E+10	2.88E+06
17	2.04	2.03E+07	4.17E+07	2.13E+07	2.22E+10	-3.5E+09	-2.10E+05
16	2.16	-2.04E+07	-4.51E+07	-2.47E+07	-2.58E+10	-4.8E+10	-2.88E+06
19	2.28	-2.03E+07	-4.17E+07	-2.13E+07	-2.22E+10	3.5E+09	2.10E+05
20	2.40	2.04E+07	4.51E+07	2.47E+07	2.58E+10	4.81E+10	2.88E+06
21	2.52	2.03E+07	4.17E+07	2.13E+07	2.22E+10	-3.5E+09	-2.10E+05
22	2.64	-2.04E+07	-4.51E+07	-2.47E+07	-2.58E+10	-4.8E+10	-2.88E+06
23	2.76	-2.03E+07	-4.17E+07	-2.13E+07	-2.22E+10	3.51E+09	2.10E+05
24	2.88	2.04E+07	4.51E+07	2.47E+07	2.58E+10	2.58E+10	1.54E+06

Table-6. Calculated transverse shear stresses.

S11	s12	S13	s22	s21	s23
6.51E+07	2.67E+06	6.77E+07	5.65E+05	-4.28E+05	1.36E+05
3.39E+07	3.09E+06	3.70E+07	5.12E+05	3.70E+05	8.83E+05
3.16E+07	-2.67E+06	2.89E+07	1.23E+06	4.28E+05	1.66E+06
6.28E+07	-3.09E+06	5.97E+07	1.28E+06	-3.70E+05	9.16E+05
6.51E+07	2.67E+06	6.77E+07	5.65E+05	-4.28E+05	1.36E+05
3.39E+07	3.09E+06	3.70E+07	5.12E+05	3.70E+05	8.83E+05
3.16E+07	-2.67E+06	2.89E+07	1.23E+06	4.28E+05	1.66E+06
6.28E+07	-3.09E+06	5.97E+07	1.28E+06	-3.70E+05	9.16E+05
6.51E+07	2.67E+06	6.77E+07	5.65E+05	-4.28E+05	1.36E+05
3.39E+07	3.09E+06	3.70E+07	5.12E+05	3.70E+05	8.83E+05
1.60E+07	-2.46E+06	1.35E+07	1.20E+06	8.27E+05	2.03E+06
6.31E+06	-5.56E+06	7.55E+05	1.14E+06	4.56E+05	1.60E+06
-2.64E+07	-5.77E+06	-3.22E+07	2.71E+05	5.73E+04	3.29E+05
-6.51E+07	-2.67E+06	-6.77E+07	-5.64E+05	4.28E+05	-1.36E+05
-6.28E+07	3.09E+06	-5.97E+07	-1.28E+06	3.72E+05	-9.14E+05
-3.16E+07	2.67E+06	-2.89E+07	-1.23E+06	-4.25E+05	-1.65E+06
-3.39E+07	-3.09E+06	-3.70E+07	-5.12E+05	-3.69E+05	-8.82E+05
-6.51E+07	-2.67E+06	-6.77E+07	-5.64E+05	4.28E+05	-1.36E+05
-6.28E+07	3.09E+06	-5.97E+07	-1.28E+06	3.71E+05	-9.15E+05
-3.16E+07	2.67E+06	-2.89E+07	-1.23E+06	-4.28E+05	-1.66E+06
-3.39E+07	-3.09E+06	-3.70E+07	-5.12E+05	-3.71E+05	-8.83E+05
-6.51E+07	-2.67E+06	-6.77E+07	-5.64E+05	4.27E+05	-1.37E+05
-5.90E+07	1.75E+06	-5.73E+07	-8.94E+05	5.85E+05	-3.09E+05
-1.93E+07	1.54E+06	-1.77E+07	-2.36E+05	1.85E+05	-5.06E+04

Graph-1. Stresses in x-z direction.

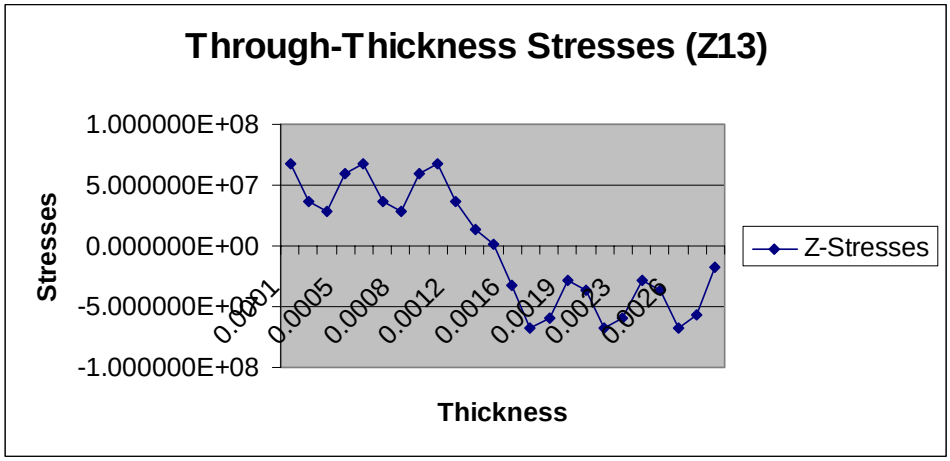

Error! No text of specified style in document.-2

Graph-2. Stresses in y-z direction.

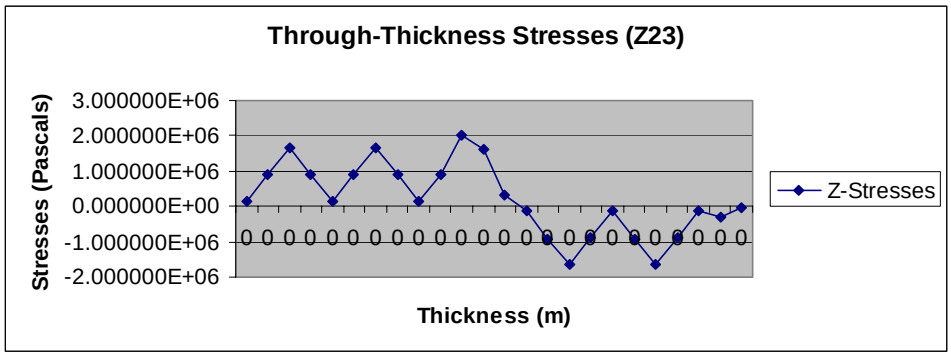

Error! No text of specified style in document.-3

Graph-3. Stresses in z direction.

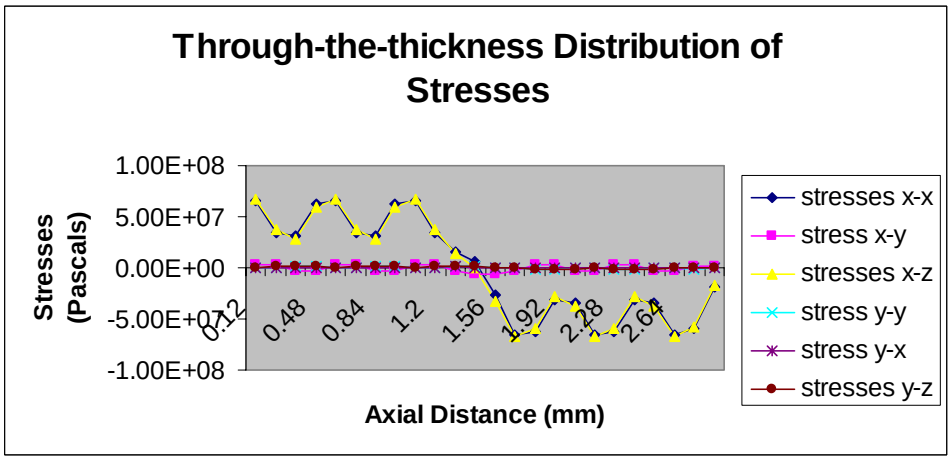

5. CONCLUSIONS

The work presents prediction of through-the-thickness stresses from 2-D model. These stresses are required to study primary damage mode (delamination) on the stiffness parameters and response on interfaces due fibre orientations and Poisson's ratios. Inter-laminar stresses combined with inherently low through-thickness strength properties in tension responsible for damage initiation and eventual structural failure. Through-thickness properties are matrix dominated and significantly lower than the in-plane stiffness and strength properties of the material from the numerical examples worked out the following observations are made: Transverse shear stresses predicted by present model when compared with three-dimensional elasticity solutions found to be reliable. The proposed procedure may be checked for other type of advanced materials and other problems or other classical boundary conditions.

Efficient and reliable computations are expected to improve the ratio of design stress to material strength, but greater advances are likely to come from improvements in fibres (higher failure strains) and matrices (greater toughness). It is necessary to assess the impact damage tolerance to improve it.

REFERENCES

[1] J.N. Reddy. 1984. A simple higher-order theory for laminated composite plates. J. Appl. Mech. 51: 745-752.

[2] M. Touratier. 1991. An efficient plate theory. Intl. J. Eng. Sci. 29(8): 901-916.

[3] R.D. Mindlin. 1951. Influence of shear on flexural motions of isotropic plates. J. Appl. Mech. 18: A31-A38.

[4] E. Reissner. 1945. Reflection on the theory of elastic plates. J. Appl. Mech. 38: 1453-1464.

[5] K.P. Soldatos. 1992. A transverse shear deformation theory for monoclinic plates. Acta Mech. 94: 195-200.

[6] Z. Kaczkowski. 1968. Plates-statistical calculations. Arkady, Warsaw.

[7] V. Panc. 1975. Theories of elastic plates. Academia. Prague.

[8] E. Reissner. 1975. On the effects of transverse shear deformation. Intl. J. Solids Struct. 25: 495-502.

[9] C.T. Herakovich. 1998. Mechanics of fibrous composites. John Wiley and Sons.

[10] Whitney J.M. 1987. Structural analysis of laminated plates. Lancaster, PA, Technomic.

[11] M. Aydogdu. 2006. Buckling analysis of cross-ply laminated beams with general b. conditions by Ritz method. Compos Sci. Technol. 66: 1248-1255.

[12] Fung Y.C. 1965. Foundations of Solid Mechanics. Prentice-Hall, Englewood Cliff, NJ, USA.

[13] Jones R.M. 199. Mechanics of Composite Materials. Taylor and Francis, Inc., Philadelphia, USA.

[14] James R. A. 2006. Impact Damage Resistance and Damage Tolerance of Fibrous Composites. PhD Thesis. Submitted at University of Bolton, UK in April.

[15] Tita I., Carvalho, J.D. and Vanepitte D. 2008. Failure analysis of composite laminates: Experimental and numerical approaches. Composite and Structures. 83: 413-428.

[16] M.K. Pandit, S. Haldar and M. Mukhopadhyay. 2007. Free vibration analysis of laminated composite rectangular plate using finite element method. J. Reinf Plast Compos. 26(1): 69-80.

[17] Meiwen Guo, E. Harik Issam and Wei-Xin Ren. 2002. Free vibration analysis of stiffened laminated plates using layered finite element method. Struct Eng. Mech. 14(3): 245-262.

[18] Kumar Khare Rakesh, Tarun Kant and Kumar Garg Ajay. 2004. Free vibration of composite and sandwich laminates with a higher-order facet shell element. Compos Struct. 65(3-4): 405-418.

[19] Y.M. Desai, G.S. Ramtekkar and A.H. Shah. 2003. Dynamic analysis of laminated composite plates using a layer-wise mixed finite element model. Compos Struct. 59(2): 237-249.